

Title

Measurement of the flood discharge of a small-sized river using an existing digital video recording system

Author names and affiliations

Ryota Tsubaki^{1*}, Ichiro Fujita², Shiho Tsutsumi²

1. Department of Civil and Environmental Engineering, Hiroshima University, Kagamiyama 1-4-1, Higashihiroshima, Hiroshima 739-8527, Japan.

2. Department of Civil Engineering, Kobe University, Rokkodai, Nada-Ku, Kobe 657-8501, Japan.

Corresponding author

* E-mail address: rsubaki@hiroshima-u.ac.jp (Ryota Tsubaki).

Tel. 81-82-424-7847, Fax 81-82-424-7847

Present address

Department of Civil and Environmental Engineering, Hiroshima University, Kagamiyama 1-4-1, Higashihiroshima, Hiroshima 739-8527, Japan.

Abstract

In this study, a closed-circuit television (CCTV) system, installed for surveillance purposes, is utilized to measure the flow rate during a flood. The procedure to determine both the angle and scale-factor of the camera is described. Then, image analysis techniques, namely the direct visual measurement method, Large-Scale PIV (LSPIV) and Space-Time Image Velocimetry (STIV), are applied to the video images recorded by the CCTV camera. The results of these methods and the conventional float measurement are compared. In addition, the accuracy of the respective methods is discussed. A set of low-quality video images of a flood during a thunderstorm that occurred under the dark ambient conditions (midnight) is analyzed using three image-based methods. The transition of the flow rate during the event is successfully estimated.

Keywords

LSPIV, STIV, Small-sized river, CCTV, river discharge measurement, float method, floating debris

1. Introduction

Compared with a large-sized river system, a small-sized river experiences runoffs of shorter duration. In the case of a local heavy rainfall hitting a small-sized river basin, an intense and concentrated run-off peak discharge is observed in the river. Furthermore, the advancement of urbanization in the basin makes the runoff duration shorter.

To forecast floods or to parameterize runoff models, a reliable data set consisting of the rainfall intensity distribution, discharge and water stage hydrographs is essential. In Japan, rating curves for the high-water period are established and maintained based on the flow rate measured by using floats (Japan river association, 1997.) Because the principle of the float measurement is simple, the measurement is robust, but its accuracy is insufficient (the error is within 10% under good conditions, Buchanan and Somers, 1969). During floods in small-sized and steep-sloped rivers, the current velocity becomes large (on the order of 5 m/s), the water surface is disturbed by the turbulence of the water and the shear by the wind, and a considerable amount of floating debris flows down. For these reasons, current-meter, ship-mounted ADCP (acoustic Doppler current profiler) or ADV (acoustic Doppler velocimetry) measurements are difficult or unsafe to conduct; thus the float method has been used to measure flow rate during floods. In the case of intense floods, the float method is also unsafe or impossible to conduct because operators have to conduct measurements at an unsafe or inaccessible site.

The river administrator utilizes the hydrological data, including rating curves in river planning, and maintains and updates them for future work. To measure flow rate and establish the rating curve, discharge measurements in both normal and flood periods are conducted. In small-sized rivers, the time lag between the start time of heavy rain-fall and the peak discharge is quite short (a few hours or less.) Moreover, the prediction of the hydrograph of rapid flooding is quite a difficult task, so the river administrator faces the dilemma of whether to perform the survey for the present flood under a limited number of surveying options. Measuring a small flood is valuable to improve the reliability of the rating curve for the range of a small discharge. However, the discharge measurement of a large flood is of significant importance to keep or to expand the applicable range of the rating curve into larger discharges (Kennedy, 1984.) The accumulation of large flood discharge data is also essential to improve the return period estimation for large and rare floods.

In recent years, a disaster prevention information system for flooding, which is a kind of Intelligent Technology (IT) system for river management, has been implemented in some large and major rivers, as well as small-sized rivers that flow through populated areas in Japan. In this system, the optical fiber network is distributed along the river. On this network, information on the water stage and rainfall intensity measured at gauging stations, the status of the riverbank displacement and the surveillance images from camera stations are provided in real time. The information is used

for a real time run-off prediction, and the result is provided to inhabitants via the Internet. The image acquisition and distribution system is called a closed-circuit television (CCTV) system. By using the optical fiber network, high quality video images recorded at many places can be broadcasted and recorded via the network. It would be quite valuable if a discharge measurement function could be implemented with the CCTV system already installed in the disaster prevention information system for a river. The discharge measurement using a CCTV system (Kruger, 2000, Creutin et al., 2003) has the advantages of safety and availability compared with other discharge measurements. Because the image data for a measurement cross-section are continuously transferred to the monitor or image server, the image can be analyzed from a safe place, and a dangerous on-site operation during the flood is unnecessary. Using an image archiving system, images during the flood can be stored automatically and analyzed after the flood. Therefore, there is no, or limited, risk of missing a chance to acquire discharge hydrographs of an infrequent large flood.

In this study, a CCTV system, already installed for surveillance purposes, is utilized to measure flood discharges of a small-sized river. It is true that the conventional float measurement has several disadvantages, namely the presence of the lead time to prepare, the limitation of observation times and the danger of the actual measurement. Most of these shortcomings of the float method can be eliminated by using the scheme developed here. The issues solved by utilizing already installed CCTV system are described in this paper. Manual and automated image analysis techniques are applied to obtain discharge data. The accuracy and applicability of these methods are compared and discussed.

2. Description of the site

The Tenpaku river basin has a drainage area of 118.8 km², which is located in the central part of Japan. The Tenpaku River originates from Mt. Sagamine and flows through Nagoya city, Aichi prefecture, before reaching the Ise Bay. The length of the main stem river is 21.5 km. Fifty-five percent of the Tenpaku river basin is composed of urban and residential areas, indicating that the basin, including an upstream land, has been urbanized. The Tenpaku river basin has suffered serious flooding damage numerous times before. After the inundation disasters that occurred on September 11, 2000, flood protection works were conducted mainly on the downstream reach. The flood protection works, completed in 2005, consisted of widening of the river width, dredging the riverbed, reinforcement of drainage pump systems and construction of a storm-water storage system. The optical fiber network and the CCTV system were also installed as part of the flood protection works implementation. Since June 2008, flood forecasts based on the hydrological record measured at the Nonami bridge station have been made. However, the cross-sectional shapes of the river and the run-off characteristics changed dramatically after the implementation of the flood protection works.

Therefore, the hydrological record of the present river system is quite limited, and the essential river engineering information, such as the rating curve for the high water period, has not been established yet due to the lack of the discharge measurement data. This data limitation is partly due to the restrictions of the float measurement described above. In this study, a CCTV camera, installed near the Nonami bridge station, was utilized for the flood discharge measurement. The Nonami bridge station is located 7.4 km from the river mouth. The width of the river is about 70 m, the mean bed elevation is about 0.3 m (in local datum level), and the mean bed slope is about 1/850 around the Nonami bridge station. The design flood discharge is 1,150 m³/s, and the design high-water level is 7.12 m at the Nonami bridge station.

3. Utilization of CCTV system

In this study, the CCTV camera, already installed for surveillance purposes, was utilized for the discharge measurement. In this context, the location and the height of the camera are fixed, and only the direction and zoom factor can be adjusted for discharge measurements. Figure 1 shows the panoramic image generated from a set of overlapping snapshots, which indicates the image area this camera is able to cover. The geometrical relationship of the camera and the river course is indicated in Figure 1. The area in Figure 1 corresponds to the section on the plan map shown in Figure 2. The camera can capture the downward stream section better. However, the resolution of the stream-wise direction of the recorded image is quite limited when shooting areas far from the camera with a low altitude angle (see, e.g., Hauet et al., 2008); therefore, the range depicted in Figure 1 and Figure 2 is an effective area for the image analysis.

The area shown in Figure 1 can be divided into the upstream, central and downstream angles. The upstream angle can observe the water surface around the bridge pier, so the water stage can be estimated quantitatively from the recorded image. The shortcoming of the upper angle is the limitation of the water surface area in the image because the bridge floor and pier cover the water surface behind them from the camera. Another shortcoming is the disturbance of the flow due to the bridge pier. The flow disturbance leads a complex flow field and makes it difficult to estimate the flow discharge. The central angle can record the water surface efficiently with higher spatial resolution. However, the effect of the flow disturbance from the bridge remains at the section recorded at the central angle. The downstream angle can also record the water surface widely with comparatively fine spatial resolution. The section recorded in the downstream angle overlaps the section used for the float measurement. In terms of the comparison with the conventional float measurement data and the consistency of the discharge data measured with the floats, the downstream angle is appropriate for use in the present case.

The recording angle should be determined on not only the geometric relationship but also

on the optical quality. As shown in Figure 3, in the case of the image angle containing a street lamp in the night time, the brightness of the image is adjusted automatically. Due to the wide range variation of the ambient luminance in the open air, an aperture of the CCTV camera is automatically adjusted. The camera tries to improve the image of the lamp and the surrounding illuminated area, and, as a result, the water surface becomes much darker in the recorded image as shown in Figure 3. With this restriction, the recording angle must not contain the street lamp to record the water surface image clearly and to conduct discharge measurement at night. To determine the recording angle, the optical quality of the images recorded at various times and in different weather condition should be surveyed. Based on the discussions above, the downstream angle was utilized for the discharge measurement with the aid of the CCTV image. The image recorded by the CCTV camera was encoded to 720 by 480 pixels, 29.97 FPS (frame per second), MPEG-2 (Moving Picture Experts Group format 2) with 6 Mbps (Mega bit per second) at the camera station. The encoded data were transferred to the image monitor or server via the optical fiber network. The original MPEG-2 data were used for real time preview. However, because the data size per frame was quite a large, stored image data were down-converted to 12 kbps MPEG-4 with 4.995 FPS. Although this procedure reduced the data volume significantly, the total data volume to storage increased with time, so the image data recorded a week before were automatically deleted. The down-conversion of the image data aimed to minimize the data size with reasonable image quality for monitoring by eye. This process deteriorated the image quality for the image analysis because of its poor resolution in both time and space.

4. Methods

There are several approaches to analyze image flow. The representative methods are PIV (Particle Image Velocimetry), PTV (Particle Tracking Velocimetry), the optical-flow method and STIV (Space-Time Image Velocimetry.) In PIV, the displacement of an image pattern in the template window is in the first image. Then, the location of the most similar image pattern in the second image is searched for. Finally, the velocity is calculated from the displacement of the image pattern from the first to second images divided by the time interval between the first and second images.

LSPIV (Large-Scale PIV. Fujita and Komura, 1994, Fujita et al., 1998) is based on the PIV technique but includes the concept of a coordinate transformation. LSPIV has been applied successfully to various rivers for measuring river flow. In PTV, the shape of each tracer particle is distinguished, and the velocity of each particle is evaluated by comparing the image pattern of the tracer particle in consecutive images. The optical-flow method is widely used in the field of the machine vision. This method solves a transport equation of the luminance distribution in the analyzing window of the sequential images to obtain the image flow velocity. In the STIV method, the one-dimensional

luminance distribution on the interrogation line is accumulated, and a two-dimensional space-time image is generated (Fujita and Tsubaki, 2002, Fujita et al., 2007.) Then, the space-time image generated is analyzed to obtain the velocity component directed to the interrogation line direction. Namely, in the space-time image, a gradient of the image pattern indicates the propagation speed of the luminance distribution on the interrogation line. Combinations of different methods, e.g., combining PIV and the optical flow method (Fujita and Tsubaki, 2004), are also suggested to achieve both robustness and accuracy in several applications.

When the surface is properly seeded by appropriate tracers (e.g., Meselhe et al., 2004), with their supplying measure or mechanism, and the image is recorded in high quality format, the LSPIV yields reliable velocity data. For the cases where naturally-arising surface image patterns caused by small fluctuation waves (e.g., Dabiri and Gharib, 2001) and the heterogeneity of the water color (Kinoshita, 1984, Utami et al., 1994, Holland et al., 1997) can be used as the flow tracer, the LSPIV or STIV methods are suitable to apply without seeding artificial flow tracers (Kim and Muste, 2005, Fujita et al. 2007). To utilize the PTV method, an image including clearly identifiable tracers is necessary because the PTV method tracks the displacement of each discrete pattern. To resolve isolable tracers in the image, PTV requires a comparatively high resolution image. To apply the PTV method for the river flow measurement, a sufficient quantity of manually seeded tracers, natural debris or stable bubble clusters are indispensable.

Available images recorded during the flood events analyzed in this study were stored in MPEG-4 format. The recorded image has a low frame rate (4.995 FPS) and low spatial resolution (354 by 240 pixels) and is subject to strong deterioration by compression noise. For this reason, the velocity distribution is estimated using the cross-correlation LSPIV method, STIV method and direct visual measurement by tracking floating objects by manual visual inspection. In LSPIV, which is used in this study, pixel displacements of the surface pattern are first analyzed using the oblique images. Secondly, the actual velocity distribution is obtained by transforming each pixel displacement in the physical coordinate by using the coordinate transformation relation. The natural water surface pattern is used to analyze the velocity in this process. The direct visual measurement is also used here because the deteriorated tracer image recorded in the poor quality format is difficult to apply in the automated PTV technique. The accuracy of the direct visual measurement for measuring the velocity of the floating object can be estimated as follows. Sample images of the floating debris and the float with light bulb are shown in Figure 4. In this figure, although the image resolution and quality are poor due to the MPEG-4 encoding, the floating debris and the float can be observed clearly, and those locations can be measured. In Figure 5, close-up samples of floating objects are depicted. As illustrated in this figure, the major part of the floating object is submerged. An error of the coordinate picked up manually in the image in the screen coordinate can be estimated as 2 pixels or smaller. The mean velocity of the target (floating debris or float) moving in the recorded angle can

be estimated as

$$\vec{u} = \frac{\vec{p_2} - \vec{p_1}}{t_2 - t_1} \quad (1)$$

where \vec{u} is the mean velocity vector of the target, $\vec{p_1}$ is the position vector of the target at instant t_1 , and $\vec{p_2}$ is the coordinate vector at instant t_2 . In the case where the target flows from right to left or vice versa, the magnitude of $\vec{p_2} - \vec{p_1}$ can be estimated as comparable to the width of the recorded image, which is 354 pixels. On the other hand, component $t_2 - t_1$ can be calculated by multiplying the recorded frame rate (4.995 FPS in the study) by the difference of frame numbers at t_1 and t_2 , so there is no error source in the evaluation of $t_2 - t_1$. Therefore, the accuracy of the estimated velocity, measured by direct visual measurement, is on the order of 1% in pixel coordinates. Meanwhile, the additional systematic error of the coordinate transformation affects the accuracy of the velocity in real coordinates. The direct visual measurement introduced here is equivalent to the flow analysis based on the Cameron effect utilized in aerial surveying (Kinoshita, 1984).

5. Results and discussions

5.1. Comparison of results between conventional float measurement and direct visual measurement.

To estimate the accuracy of the direct visual measurement, images recorded during the conventional float measurement conducted by the surveying company were analyzed by the direct visual measurement, and the results were compared. In Figure 6, the stream-wise velocities of the eight floats with the bulb thrown at around 2:00 am, June 16, 2006 during the peak discharge of about 250 m³/s are compared. This flood occurred before determining the proper shooting angle, so the image was taken at the upstream angle (see Figure 1). Because of this inappropriate condition, the cross-sections used in the float measurement and image analysis were not identical (see Figure 2). Therefore, some variation can be observed in Figure 6 ($r^2 = 0.76$), but the overall agreement is favorable ($y = 0.969x$). Obviously, the float result contains an error, so it is difficult to discuss the absolute accuracy using only the data available. However, at least from the result shown in Figure 6 and from the principles of the direct visual measurement and the float measurement, the accuracy of the tracer velocity measured by the direct visual measurement had the same or smaller error compared with the result by the conventional float measurement. This was because the conventional float measurement was conducted completely on site and by eye, but the direct visual measurement

analyses recorded images. Thus, the direct visual measurement was superior in terms of both spatial and temporal accuracies.

5.2. Discharge measurement using direct visual measurement.

The discharge hydrograph during the flood with its peak discharge of about 330 m³/s that occurred around 1:00, August 29, 2008 was estimated using the CCTV image and the direct visual measurement technique. Figure 7 depicts the water stage hydrograph at this event recorded at the Nonami bridge station. The water stage began to rise rapidly from 23:30, August 28 and reached its peak at 4.66 m after about 1.5 hours, namely at 1:10, August 29. Afterwards, the water stage decreased gradually to a normal level except for a small second peak observed at 5:00. The recorded image was shot with the downstream angle as shown in Figure 8. This angle was determined based on the discussion in Section 3, namely taking into account of the geometrical conditions, the optical quality under different ambient conditions and the correspondence of the measurement section used in the conventional float measurement.

Figure 9 shows a recorded image at 1:00, August 29. The locations of wooden debris clusters are presented. The density of wooden debris changed with time and was generally proportional to the water stage and flow rate at the rising stage. During the 15 minutes around the peak discharge, more than 21 clearly visible clusters of wooden debris can be observed. In the Tenpaku River, a sufficient amount of the wooden debris flowed down during the flood, so it could be used as natural tracer during the flood (Bocchiola et al., 2002, Comiti et al., 2006, Nihei and Wakatsuki, 2010) in this river.

In Figure 10, the trajectories at 2-second intervals of the wooden debris observed during 15 minutes around the peak discharge are plotted. Due to the high density of the wooden debris, ten tracers (from 21 tracers) are picked up and depicted in this figure. Because there is a wide range of the cross-sectional locations of the trajectories, the velocity distribution at the cross-section can be estimated. After the mean drift velocity of each floating debris cluster is calculated using Equation 1, a velocity correction factor of 0.85 (Aki, 1932) is multiplied with the debris velocity to evaluate the depth averaged velocity. While the velocity correction factor changes depending of the bed roughness, the levels of turbulence and the unsteadiness of the flow, a universal approach to determine the velocity correction factor has not been established yet, so the standard value 0.85 was used for all surface image velocimetries (direct visual measurement, LSPIV and STIV) in this study. To calculate the discharge, the river cross-section was divided by 10-m intervals into 6 parts. Then, the mean velocity at each divided cross-section was calculated, and the total flow rate was calculated by the summation of the partial discharge at each divided cross-section. It was confirmed that the total flow rate was insensitive to the number of cross-sectional divisions. The division number of 6 is

consistent with the number of cross-section divisions used in the conventional float measurement, so the same division was utilized in this analysis.

Figure 11 shows the relation between the water stage and the discharge (rating curve) during the flood event at August 29, 2008. The flow rate was estimated at 30-minute interval from 24:10 to 2:10, and one to two-hour intervals from 2:10 to 7:10. This event was the largest flood event after the implementation of the flood protection works. In this regard, this flood event is of great importance to comprehend the hydrological properties of the revised river system. However, the conventional float measurement was not conducted in this event due to the emergent occurrence of the flood and the shortage of the lead time to set up the measurement. By using the CCTV system and the image analysis technique, the detailed rating curve for the rapid flood event of the small-sized river system could be successfully established, as shown in Figure 11.

Figure 12 compares the rating curves of the August 29, 2008 event analyzed by the image technique and the June 16, 2006 event obtained by the float measurement. Unfortunately, the rating curve for the June 16, 2006 event contained only a lowering phase because of the delay of the start of the float measurement. The image recorded in June 16, 2006 was shot at the upstream angle, and, therefore, the image contains quite a limited area of water surface with dark color, which made it impossible to estimate the rising stage hydrograph from the water surface image. Compared with the curve of the 2006 event, the falling phase of the 2008 results showed a smaller discharge at the equivalent water stage because of the change of river morphology due to the vegetation settlement and the sedimentation. The cross-sectional widening and dredging around the measuring cross-section was completed in 2005, so the cross-section of 2006 had a larger discharge capacity. However, due to the vegetation settlement and bathymetry changes within two years after the river works (compare downstream sections of Figure 1 and Figure 3), the flow capacity had been reduced, and those changes caused a transition of the rating curve, as shown in Figure 12 quantitatively.

5.3. Comparison of discharges obtained from LSPIV, STIV and direct visual measurement

The results above were based on the direct visual measurement. The direct visual measurement was introduced due to the poor quality of the stored image. However, in practical applications, automated estimation of the flow discharge is preferable or required. The LSPIV and STIV analyses were conducted here to obtain the surface velocity distributions and the flow rates for the August 29, 2008 event. The fundamental parameters of the LSPIV analysis (Okabe et al., 2007) and STIV analysis (Fujita et al., 2007) are described in Tables 1 and 2, respectively. In Figure 13, the flow rates estimated by LSPIV, STIV and direct visual measurement are compared. The correlations between the direct visual measurement and two automated results are strong (the coefficients of determination R^2 are 0.96 for both), which indicates that the LSPIV and STIV results can be used to

predict the flow rate instead of the direct visual measurement and the float measurement because the direct visual measurement and the float measurement are similar in principle. In quantitative terms, the LSPIV discharge underestimate was 26% compared with the direct visual measurement result, while the STIV discharge underestimate was 9% compared with the direct visual measurement. In the direct visual measurement, the clusters of clearly identifiable debris were used as surface tracers, but the LSPIV and STIV tracked more general image patterns of the water surface and had many error sources related to image properties and quality (Kim and Muste, 2005, Hauet et al., 2008.) The correlation of surface water velocity and the floating debris velocity is comparatively unambiguous; however, there is an uncertainty in the association between the surface flow and the general image flow. Due to the difference in the image analysis procedure used in the three visual techniques, the direct visual measurement showed the more probable water surface velocity.

The reason of the underestimation in the LSPIV and STIV results may be related to the steady components of the image due to the reflection of the opposite side bank scene, the surface waves caused by the standing wave and the bursting at specific points (Jackson, 1976) due to the inhomogeneity of the river bed shape and flow. These steady components of the image have a comparatively large spatial scale (e.g., Fox and Belcher, 2009), and the patterns do not drift downstream but fluctuate with time. The steady components affect LSPIV and STIV analyses and cause the underestimation of the surface velocity.

The magnitude of underestimation in flow rate of LSPIV (26%) was larger than that of STIV (9%), perhaps because LSPIV is more sensitive to the details of the surface pattern of the instantaneous image than STIV, which analyzes the consistent pattern drift in the space-time dimension and is tolerant of instantaneous noise (Fujita and Tsubaki, 2002.) The substantial underestimation of LSPIV was due to the limitation of the image resolution. Additionally, the flood occurred at night, and the ambient light was quite dark. In such conditions, the CCTV camera recorded images in the frame accumulation mode, which integrates the luminance distribution for a specific time duration (a few frames) to cover the shortage of the luminance for each instant frame. This technique acts as a kind of time filter, reduces the spatial and temporal resolutions of image and causes the interruption of the proper image pairing in LSPIV analysis.

It is expected that the improvement of the stored image quality will reduce the error of the automatically obtained discharge information, so quantitative evaluation of the effect of image quality including the encoding method and ambient conditions in the image based methods should be examined. Further investigation should be conducted to verify the applicability of the utilization of the natural surface tracer for continuous and stable discharge measurements. In particular, the relation of the micro-scale and the coherent structures of the flow to the surface fluctuation and the surface image pattern should be explored.

Table 1. LSPIV parameters

Interrogation window size (pixel)	19 by 11
Searching window (pixel)	-1 to 15 in horizontal, -6 to 2 in vertical
Frame intervals (sec)	1.0
Minimum correlation (-)	0.5
Number of image pair (-)	95

Table 2. STIV parameters

STIV image size (pixel)	245 in space 299 in time
Pixel size (m/pixel)	0.1
Frame intervals (sec)	0.2
Interrogation window size (pixel)	50 by 50
Pre-process image filtering	Gaussian with $\sigma=0.3$

Conclusions

A CCTV system, installed for surveillance purposes, was utilized for measuring the flow rate during floods. The procedure to determine both the angle and scale-factor of the camera is described. Then, image analysis techniques, namely the direct visual measurement, LSPIV, and STIV, were applied to the video images recorded by the CCTV camera, and the results of those methods and the conventional float method were compared. The accuracy of the respective methods is discussed. A set of low-quality video images, recorded during a flood in a thunderstorm that occurred under the dark ambient conditions (midnight), was analyzed using three image-based methods, and the transition of the flow rate during the event was successfully estimated. By using the CCTV image and image analysis techniques, the continuous measurement of the flow discharge from start to end of the rapid flood event could be achieved.

Utilization of CCTV images for discharge measurements is a useful tool to establish a rating curve and has strong potential as an alternative to the conventional flow rate measurements. Further observations comparing discharges obtained with the CCTV utilization and other discharge measurements (e.g., using the acoustic Doppler profiler) should be conducted to clarify the applicability of the discharge measurement using CCTV in a wide range of flow and weather conditions.

Acknowledgments

The authors would like to thank Dr. S. Mama, Mr. H. Takemura and Mr. K. Yamashita of Yachiyo Engineering Co., Ltd. and Mr. K. Kinnbara of Aichi Prefecture for providing essential data for this study.

References

- Aki, K., 1932. On correction coefficient of the measured velocity of float, specially of float rod, to the mean velocity of flow in a vertical, *Civil Engineering, JSCE*, 18(1), 105-129.
- Bocchiola, D., Catalano, F., Menduni, G., Passoni, G., 2002. An analytical-numerical approach to the hydraulics of floating debris in river channels, *Journal of Hydrology*, 269, 65-78.
- Buchanan, T. J., Somers, W. P., 1969. Discharge measurements at gauging stations. In *Techniques of Water Resources Investigations, Chapter A8, Book 3, Applications of Hydraulics*, USGS.
- Comiti, F., Andreoli, A., Lenzi, M.A., Mao, L., 2006. Spatial density and characteristics of woody debris in five mountain rivers of the Dolomites (Italian Alps), *Geomorphology*, 78, 44-63.
- Creutin, J.D., Muste, M., Bradley, A.A., Kim, S.C., Kruger, A., 2003. River gauging using PIV techniques: a proof of concept experiment on the Iowa River, *Journal of hydrology*, 277, 182-194.
- Dabri, D., Gharib, M., 2001. Simultaneous free-surface deformation and near-surface velocity measurements, *Experiments in fluids*, 30, 381-390.
- Fox, J.F., Belcher, B.J., 2009. Comparison of LSPIV, ADV and PIV data that is decomposed to measure the structure of turbulence over a gravel-bed, In *proc. of 33rd IAHR congress*, Vancouver, Canada.
- Fujita, I., Komura, S., 1994. Application of video image analysis for measurements of river-surface flows, *Annual Journal of Hydraulic Engineering, JSCE*, 38, 733-738 (in Japanese).
- Fujita, I., Muste, M., Kruger, A., 1998. Large-scale particle image Velocimetry for flow analysis in hydraulic engineering applications, *J. Hydraulic Research*, 36(3), 397-414.
- Fujita, I., Watanabe, H., Tsubaki, R., 2007. Development of a non-intrusive and efficient flow monitoring technique: the space-time image Velocimetry (STIV), *Int. J. River Basin Management*, 5(2), 105-114.
- Fujita, I., Tsubaki, R., 2002. A novel free-surface velocity measurement method using spatiotemporal images, In *proc. of Hydraulic Measurements and Experimental Methods*, on CD-ROM.
- Fujita I., Tsubaki, R., 2004. Measurements of vorticity field from river flow images, *Int. Conf. on Advanced Optical Diagnostics in Fluids Solids and Combustion*, V0032, Tokyo, Japan.
- Holland, T., Holman, R.A., Lippmann, T.C., 1997. Practical use of video imagery in nearshore oceanographic field study, *IEEE J. Oceanic Engineering*, 22(1), 81-95.

- Hauet, A., Creutin, J.-D., Belleudy, P., 2007. Sensitivity study of large-scale particle image Velocimetry measurement of river discharge using numerical simulation, *J. Hydrology*, 349, 178-190.
- Jackson, R.G., 1976. Sedimentological and fluiddynamic implications of the turbulent bursting phenomenon in geophysical flows, *J. Fluid Mech*, 77(3), 531-560.
- Japan river association (ed.), 1997. Manual of technical standard for river engineering and sediment control, investigation part, 33-58.
- Kennedy, E. J. 1984. Discharge ratings at gauging stations. In *Techniques of water-resources investigations*, Chapter A10, Book 3., Applications of Hydraulics, USGS.
- Kim, Y., Muste, M., 2005. Uncertainty analysis of mobile large scale PIV, IIHR short note.
- Kinoshita, R., 1984. Present status and future prospects of river flow analysis by the aerial photograph, *J. Hydraulic, Coastal and Environmental Engineering, JSCE*, 345 (II-1), 1-19 (in Japanese)
- Kruger, A., Bradley, A., Muste, M., Fujita, I., 2000. Real-Time Measurements of Free-Surface Velocity Using Imaging Techniques, *Hydroinformatics 2000*, on CD-ROM.
- Meselhe, E.A., Peeva, T., Muste, M., 2004. Large scale particle image Velocimetry for low velocity and shallow water flows, *J. Hydr. Engrg.*, 130(9), 937-940.
- Nihei, Y. and N. Wakatsuki, 2010. Field measurement of floating-litter transport in a river under flooding conditions, *J. Hydraulic, Coastal and Environmental Engineering, JSCE*, 66(1), 19-24.
- Okabe, T., Fujita, I., Tsubaki, R., Wakuda, A., 2007. Standard for application method of LSPIV applied to surface video record of actual flood flow, *Annual Journal of Hydraulic Engineering, JSCE*, 51, on CD-ROM (in Japanese).
- Utami, T., Ueno, T., 1994. Analysis of flood flows by photograph image processing, *J. Hydraulic, Coastal and Environmental Engineering, JSCE*, 503(II-29), 1-17 (in Japanese)

Figure captions

Fig. 1. Panoramic image generated from the view of the CCTV camera near the Nonami bridge station.

Fig. 2. Plan map around the Nonami bridge and viewing area of the panorama image of Fig. 1.

Fig. 3. Images recorded under different ambient conditions.

Fig. 4. Sample snap shots of the float with a light bulb and the debris cluster.

Fig. 5. Close-up samples of floating objects.

Fig. 6. Comparison of the float measurement velocity and direct visual measurement velocity.

Fig. 7. Discharge hydrograph of the flood event at the Nonami bridge station on August 29, 2008.

Fig. 8. Viewing angle of downstream angle used to record the August 29, 2008 event and its positional relation to the float measurement cross-sections.

Fig. 9. Sample snap shot of August 29, 2008 flood event. The arrows indicate location of some debris clusters.

Fig. 10. Trajectory plots of the debris clusters observed during 1:10 to 1:35 of the August 29, 2008 event. Each circle shows the instantaneous location at 2-second intervals.

Fig. 11. Discharge rating curve for the August 29, 2008 event based on direct visual measurement results.

Fig. 12. Comparison of rating curves for the July 16, 2006 event (based on the float measurement) and for the August 29, 2008 event (based on direct visual measurement results).

Fig. 13. Comparison of discharges obtained by direct visual measurement and two automated analysis results by LSPIV and STIV.

Figure 1

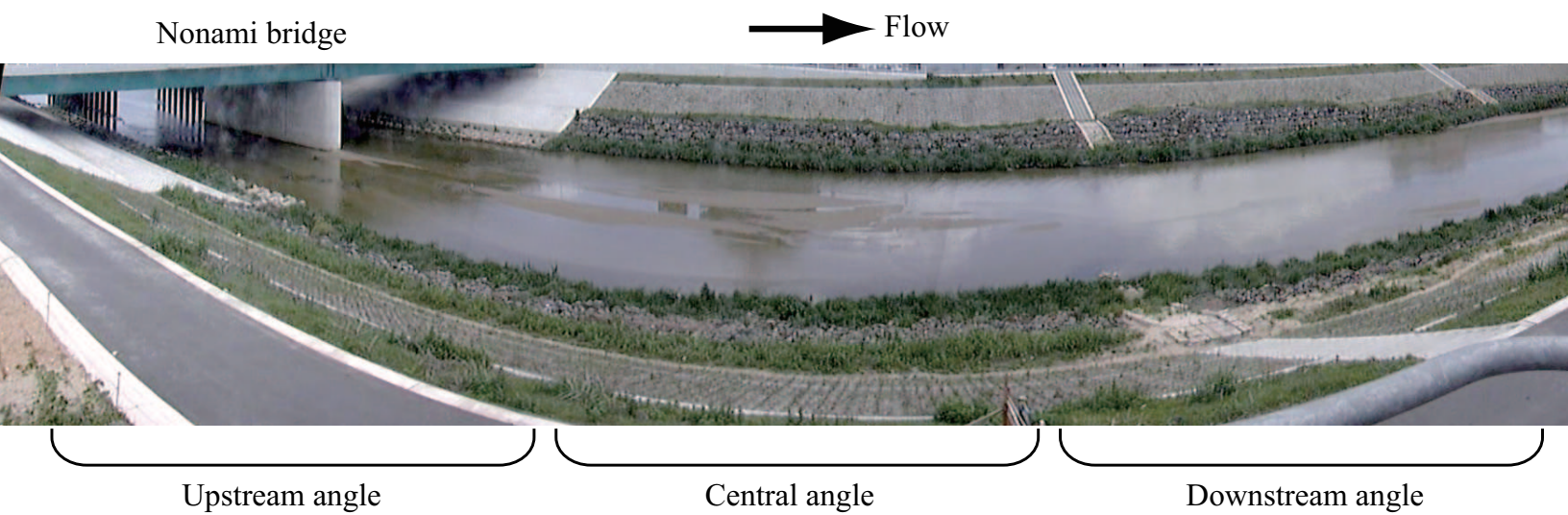


Figure 2

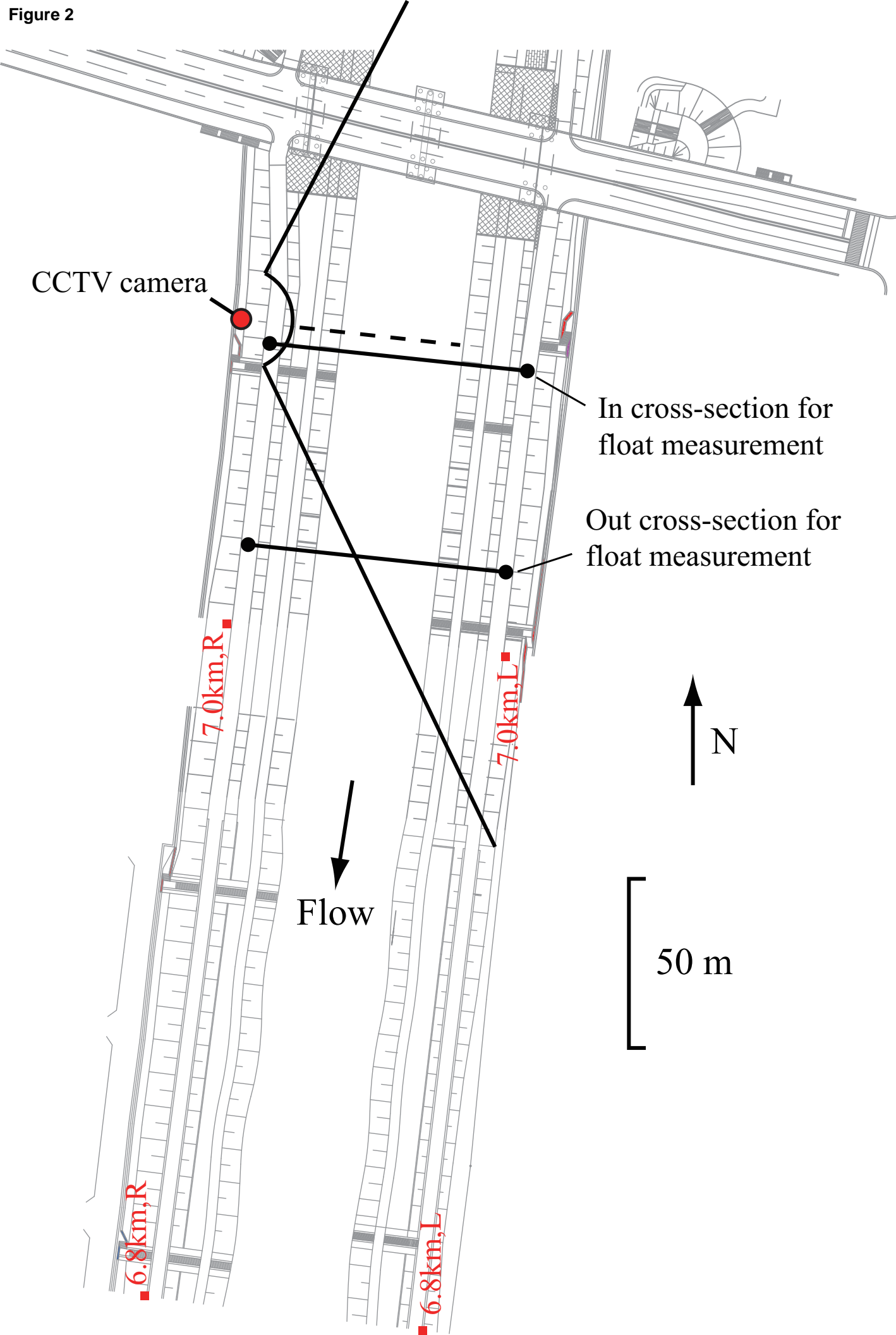


Figure 3



(a) Cloudy (Day, June 16, 2006)



(c) Cloudy (Day, August 28, 2008)

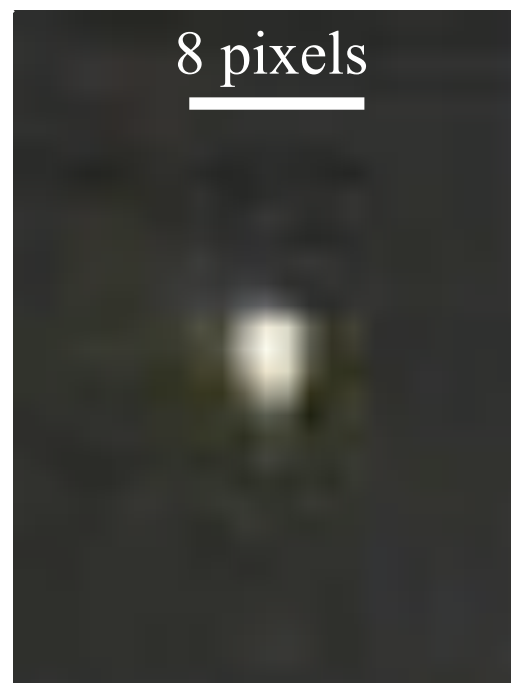


(b) Rain (Night, June 16, 2006)

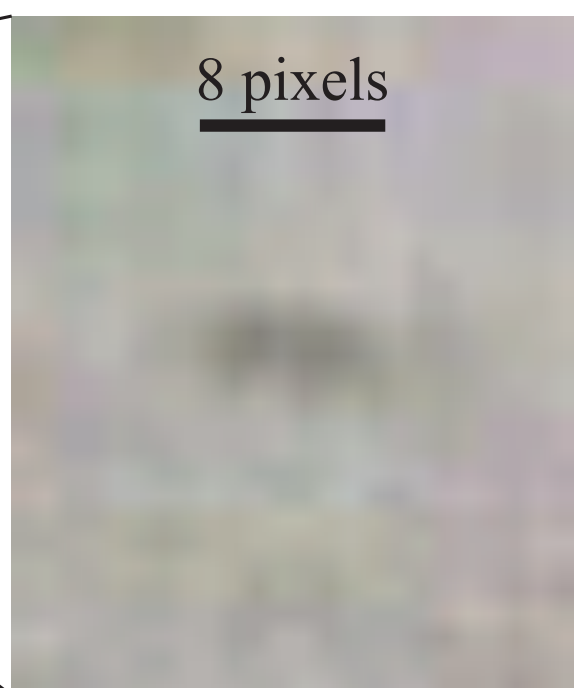
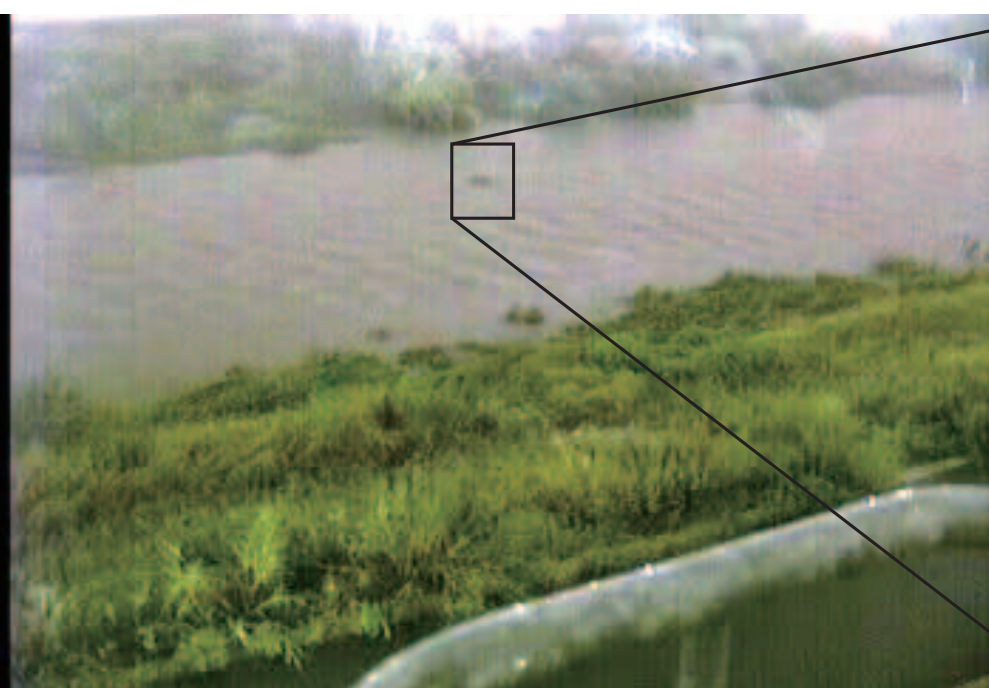


(d) Thunder storm (Night, August 29, 2008)

Figure 4



(a) Sample image of a float with light bulb



(b) Sample image of a debris cluster

Figure 5

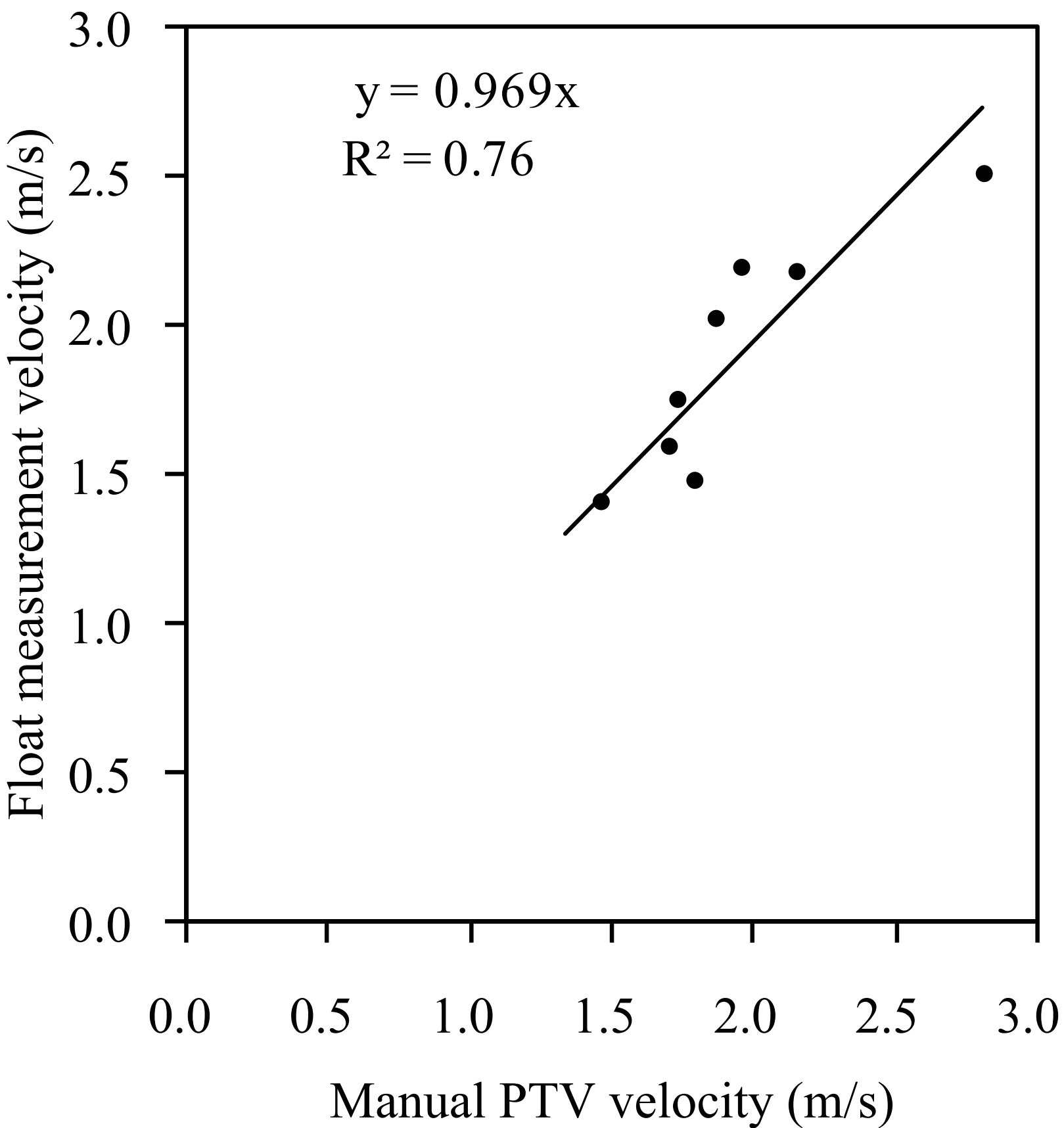


Figure 6

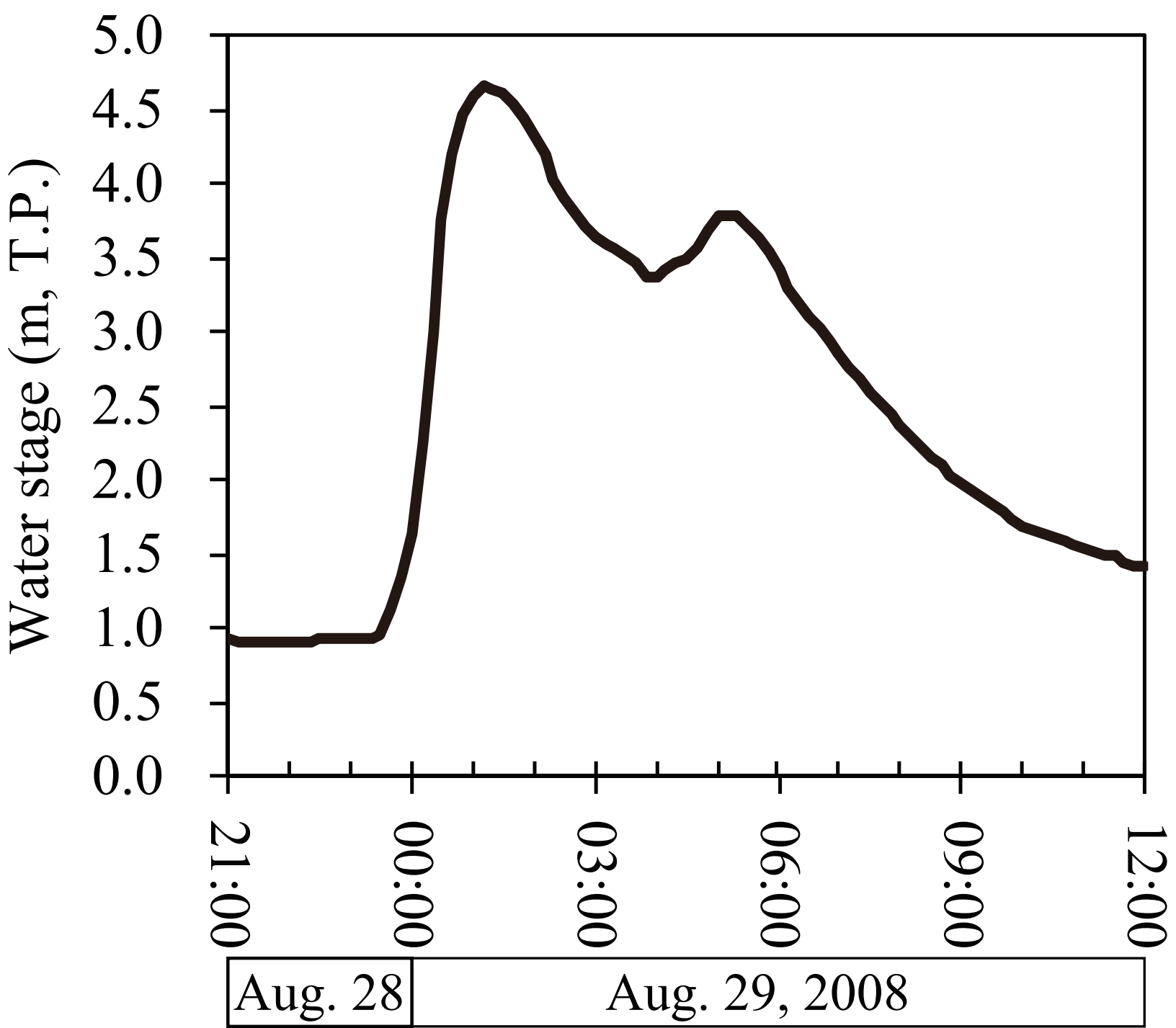


Figure 7

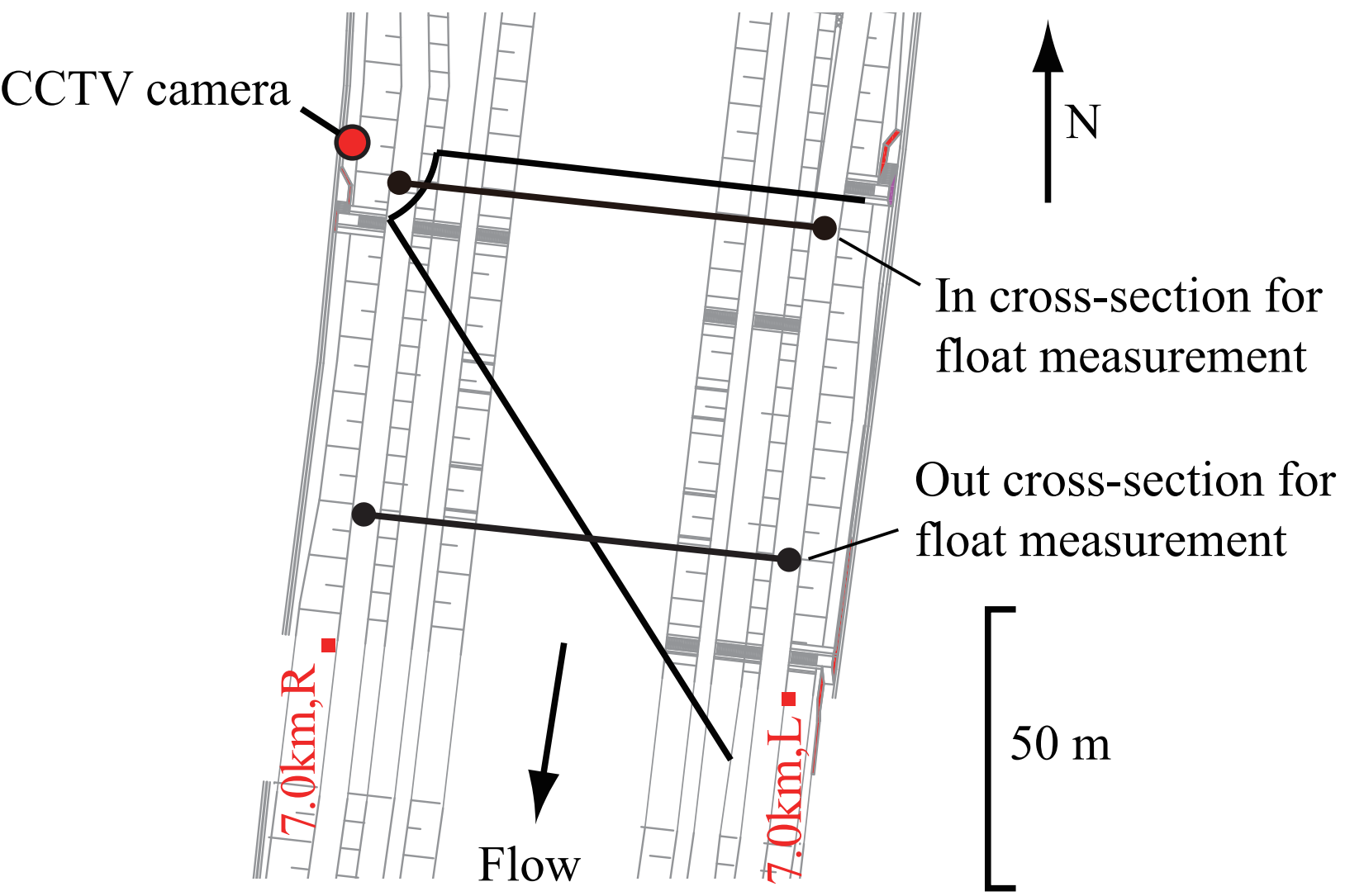


Figure 8



Figure 9

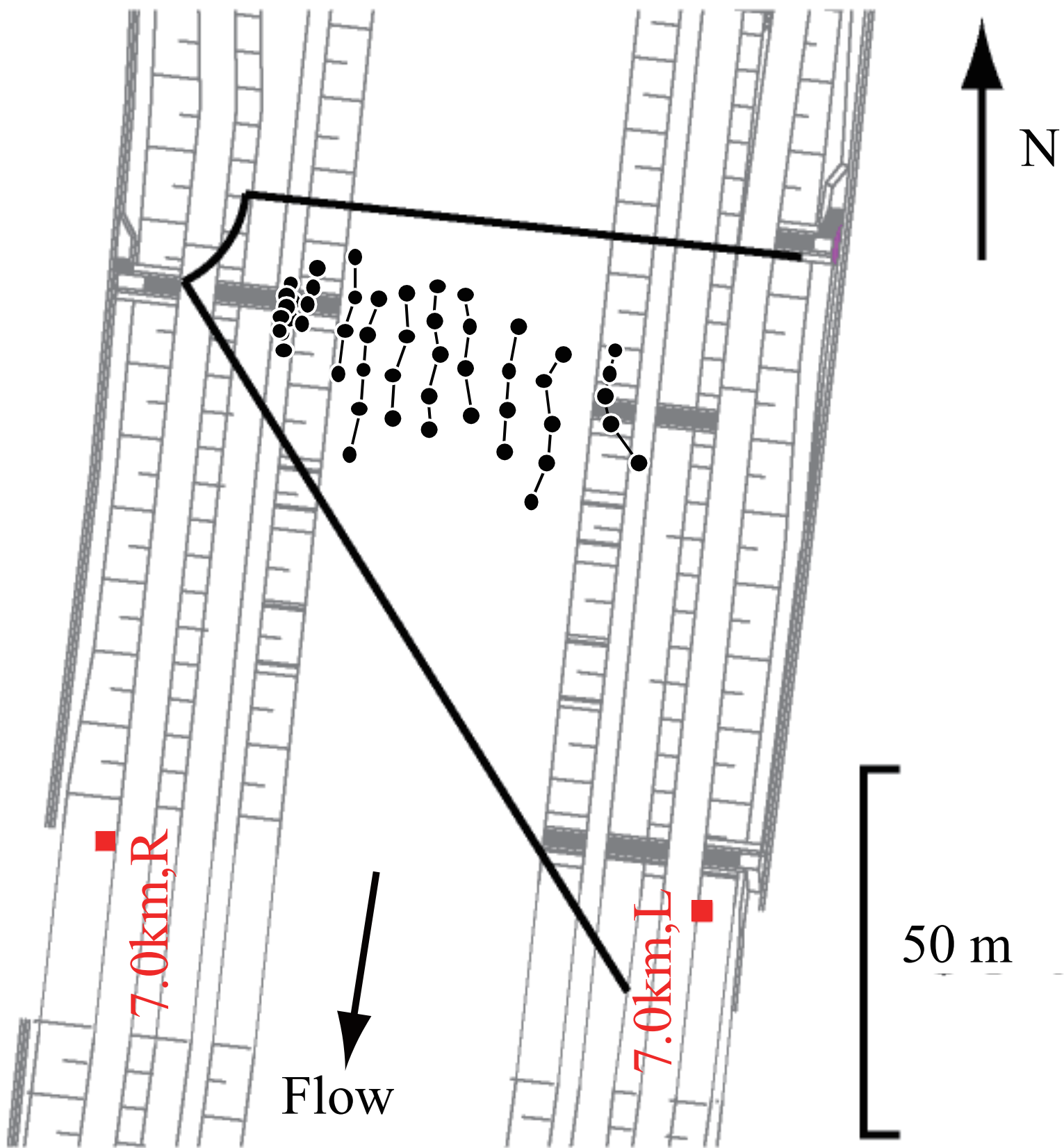


Figure 10

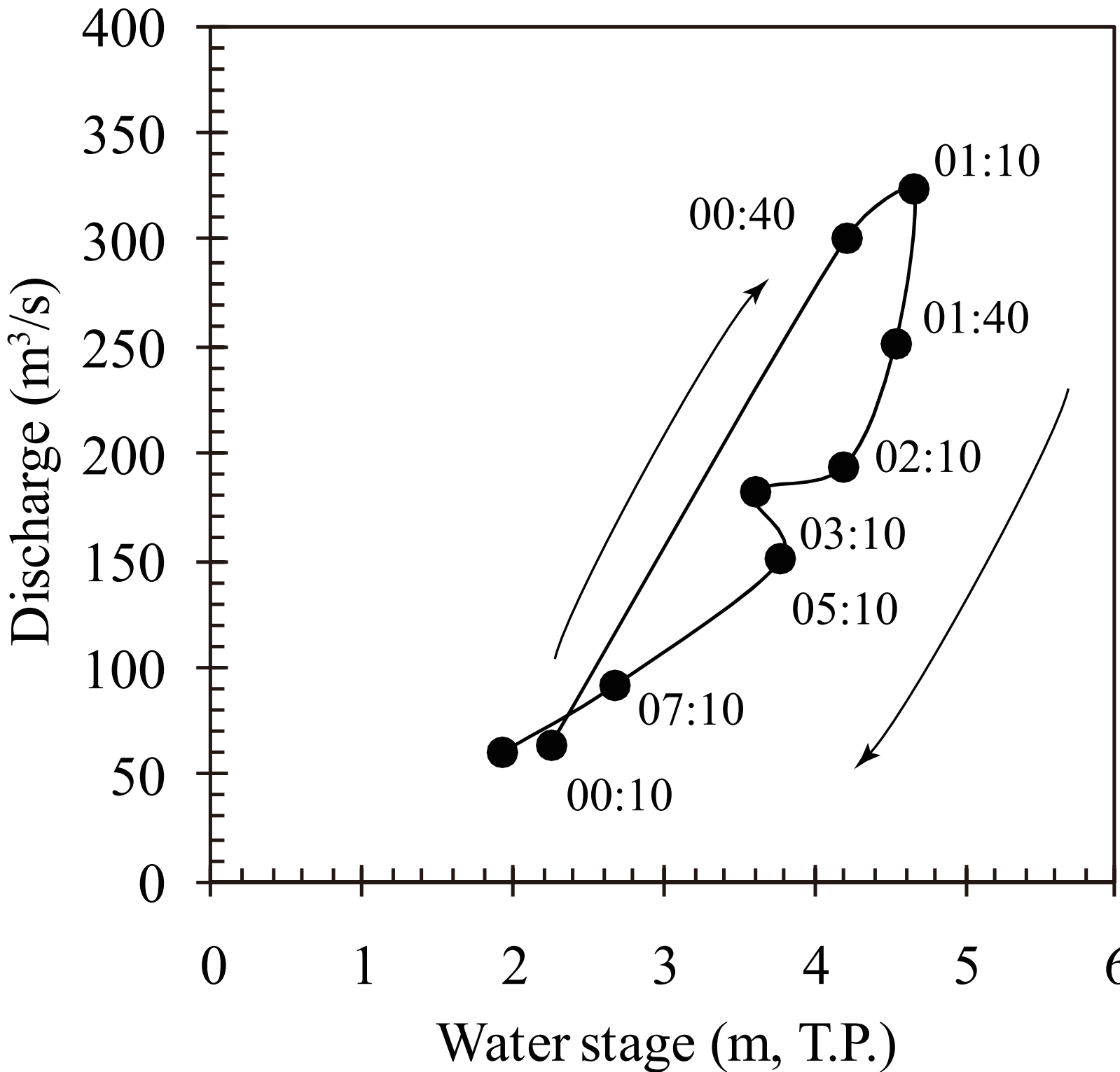


Figure 11

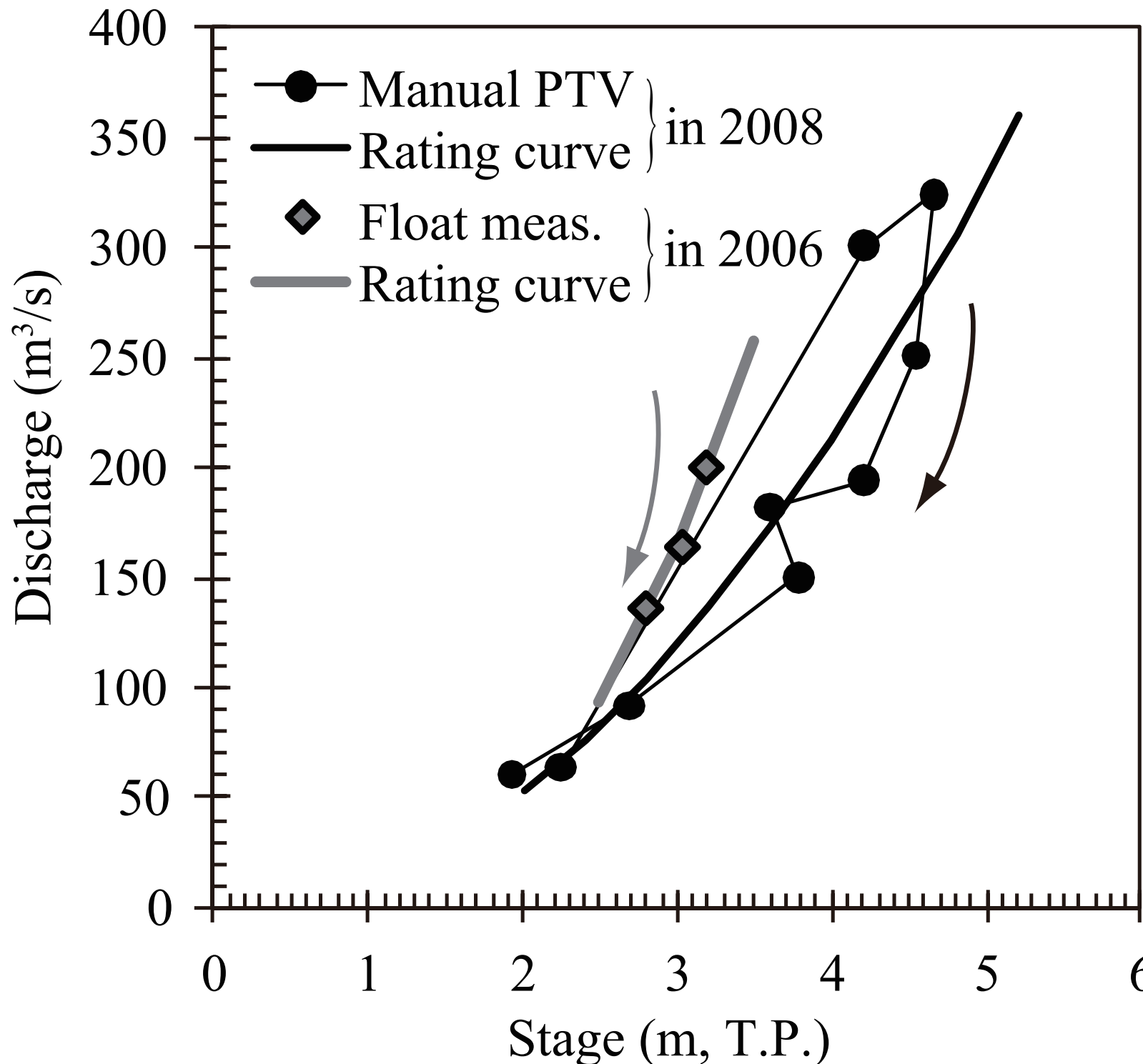


Figure 12

